
Performance of the H.E.S.S. cameras.

P. Vincent¹, J.-P. Denance¹, J.-F. Huppert¹, P. Manigot², M. de Naurois², P. Nayman¹, J.-P. Tavernet¹, F. Toussenel¹, L.-M. Chounet², B. Degrange², P. Espigat³, G. Fontaine², J. Guy¹, G. Hermann⁴, A. Kohnle⁴, C. Masterson⁴, M. Punch³, M. Rivoal¹, L. Rolland¹, T. Saitoh⁴, for the H.E.S.S. collaboration.

(1) LPNHE, IN2P3/CNRS Universités Paris VI & VII, Paris, France

(2) LLR, IN2P3/CNRS Ecole Polytechnique, Palaiseau, France

(3) PCC, IN2P3/CNRS College de France, Paris, France

(4) Max Planck Institut fuer Kernphysik, Heidelberg, Germany

1. Introduction

The H.E.S.S. experiment is a new generation ground-based atmospheric Cherenkov detector. The first phase of this experiment consists of a square array of four telescopes with 120-metre spacing. Each telescope, equipped with a mirror of 107 m², has a focal plane at 15 metres where a camera is installed. Each camera consists of 960 photo-multipliers (PMs), providing a total field of view of 5°, with the complete acquisition system (analogue to digital conversion, read-out, fast trigger, on-board acquisition) being contained in the camera. The cameras of the H.E.S.S. telescopes are currently being installed in the Khomas highlands, Namibia. The first telescope has been taking data since June, 2002 and the second since February, 2003. Stereoscopic coincident trigger mode should begin in June, 2003 and full Phase I operation should be underway early in 2004. The performance of the cameras will be presented and their characteristics as measured during data taking will be compared with those obtained during the construction phase using a test bench. Future upgrades based on experience operating the two first cameras are also discussed.

2. The cameras of the H.E.S.S. telescopes.

A camera is approximately octagonal, fitting in a cylinder 2 metres in length and 1.6 metres in diameter, and weighing about 900 kg (see Fig. 1). The front part contains 60 interchangeable modules (“drawers”) with 16 PMs each, lodged in a “pigeon-hole” plate. The drawers are held by only two screws and can be easily extracted from the body of the camera to be replaced by a new drawer. Each drawer communicates with the rest of the electronics through three connectors at the rear, which plug in automatically when drawers are installed.

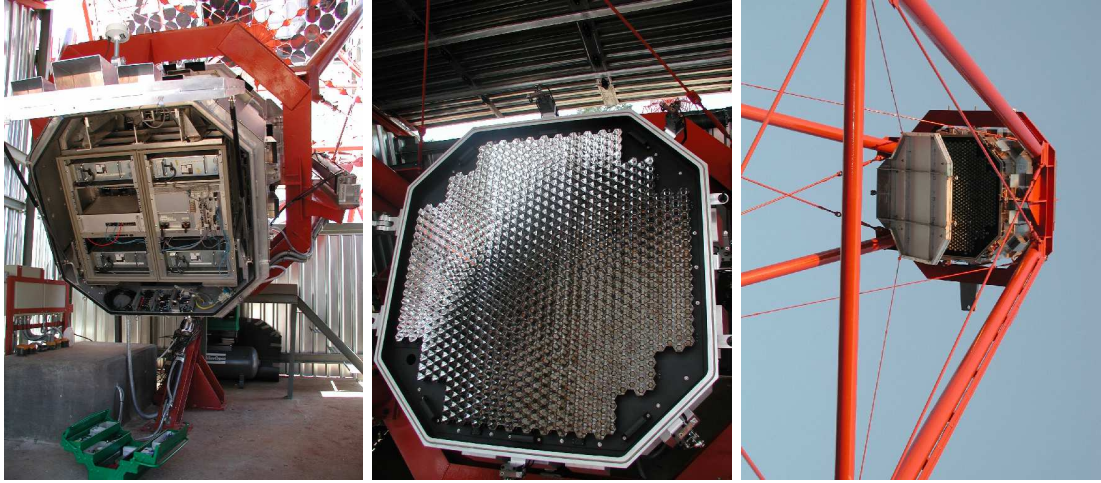


Fig. 1. View of the second H.E.S.S. camera. The picture on the left shows the rear with the four power supplies, the mixed crate incorporating the custom bus and compact PCI bus, and the network interface. The central picture shows the front side of the camera with lid open showing the 960 Winston cones. On the right we see the camera on the telescope.

This conception allows an easy access for tests and repairs of the camera electronics. In front of the drawers, a plate in three sections holds individual Winston cones for each PM which concentrate the Cherenkov light in the central region of the photo-cathode where the quantum efficiency is at a maximum of about 30%. These cones allow the collection of about 75% of the photons reflected from the mirror. They also considerably reduce the background contribution from albedo by limiting the PM's field of view to the angular size of the mirror. In the rear of the camera, an electronics rack is equipped with four power-supply crates, the camera acquisition and control systems, and the network interface. This rack can be slid out on rails from the camera body to access the cables and connectors between front and back side of the camera. Lastly, only three cables come from the camera to the ground: a copper cable for the current, one optical fibre for the network, and an other fibre for communications with central trigger.

3. The electronics.

The electronics of the camera consist of a front-end contained in the drawers which includes the readout and first-level trigger and a second section with the local acquisition system mentioned above. Drawers contain 16 PMs, each powered by an active base. These bases provide a high voltage of more than a thousand volts calibrated to generate a signal of 2×10^5 electrons for each photon converted at the photo-cathode. The PMs use a borosilicate window and provide

a 20–30% quantum efficiency in the wavelength range 300–700 nm.

The readout channel takes advantage of analogue memories ARS0 (“Analog Ring Sampling memory”) developed for the ANTARES experiment by the CEA/DAPNIA-SEI. These memories sample the signal at 1 GHz and store it in 128 cells while awaiting the trigger decision. The pulse from each PM is divided between two channels with different amplification factors. A high-gain channel, for low signal amplitudes, gives a dynamic range from 1 to about 100 photo-electrons. Before this upper limit, at around 16 photo-electrons, the low gain channel can measure a signal up to 1600 photo-electrons. The overlapping region allows inter-calibration between both channels. The signal from a triggered event is read from the analogue memory in a window of 16 samples and then digitized with a 12-bit ADC and stored in an FPGA chip. The samples can be saved for an analysis of the pulse shape or integrated directly in the FPGA so as to transmit and save only the total charge in a pixel. The readout-window size is a programmable parameter that can be changed as a function of future studies.

The local camera trigger is based on two parameters: the number of photons arriving in a pixel and the identification of a concentration of signal in a part of the camera. To construct the latter criterion the camera has been divided in 38 sectors of 64 PMs with logic on cards contained in the rear crate. Sectors overlap with their neighbours to prevent local inhomogeneities which would result from a shower image arriving in the boundary between two sectors. The time needed to build the trigger signal is about 70 ns, which is fast enough permit reading of the signal stored in the ARS0. A card dedicated to the trigger management (“GesTrig”) sends a signal through two fanout cards to the 480 analogue memories. The memories stop acquiring data, a programmable pointer identifies the region of interest given the trigger-signal formation time, and the readout of the data starts. The time until the converted signals are ready in the drawers’ FPGAs is measured to be 270 μ s after the shower’s arrival, and is remarkably stable.

The interface with central trigger of the multi-telescope system is performed via a local module embedded in the camera. This central trigger interface is connected to the GesTrig trigger manager card and informs the central trigger of the current status of the camera with a “busy” signal. If there is no coincidence with other telescopes, the central trigger returns a “fast clear” within a couple of μ s, which is sent to the GesTrig and thence to the drawers to stop the readout of the analogue memories and to reset the drawers.

4. Data acquisition architecture and performance

The acquisition system is based on the use of the new Compact-PCI (cPCI) norm that allows 64-bit word transfer at 33 MHz. A second bus (CustomBUS) within the data acquisition crate is dedicated to the configuration of the sectorization of the trigger. The drawers are connected to the acquisition by 4 final buses

(Box-Bus), and when an event is available for transfer they send a request to a card holding FIFO memories (FIFO-card) located on the cPCI bus. This card plays the rôle of master and controls the transactions on the 4 buses by sending acknowledges to slaves (drawers). All buses accept asynchronous transfer, and the full data transfer from the 15 drawers present on each bus is completed after $340 \mu\text{s}$. This year, the RIO-4065 processor from CES has been installed on the first two cameras. This new processor is able to perform direct access between a card in the cPCI bus and its own memory and so improve the performance of the acquisition. The FIFO memories are read-out through the cPCI bus by a DMA chip that transfers the full camera's data in less than $140 \mu\text{s}$. This last time, together with the bus transfer time and the ARS conversion time of the previous section, defines the dead-time of the acquisition. As the readout time of the FIFO memory is lower than the other times, this task can be parallelized so that the dead-time for a camera is $610 \mu\text{s}$, corresponding to a maximum acquisition rate of 1.6 kHz which represents an improvement of a factor of three from the initial camera's performance. Under these conditions, at a typical trigger configuration of 4 pixels at 5 photo-electrons, the observed counting rate is 250 Hz. This rate gives a dead-time of about 14%, compared to 30% with the initial camera.

The data acquisition system (DAS) in the camera is build around the Linux operating system and written in C. This system controls the behaviour of the overall camera: one card controls the camera lid operation, the 95 fans and 16 temperature sensors; a GPS card for time stamps receives interruptions from the GesTrig trigger card; a CAN bus interface controls the four power-supply crates; an I/O card manages the trigger; a mezzanine card located on the CustomBUS receives some serial event data the from central trigger interface (event number ...). Data are transfered from the local CPU to the central DAS via a 100 Mbits/s network for conversion and storage in ROOT format.

5. Conclusion.

Since the installation of the first camera “prototype” several upgrades have been carried out. Experimentally we had strong indications that noise from the switching power-supplies considerably disturbed the data “traffic” on the BoxBus. The buses on new camera have been modified to remedy this problem and the first prototype has been upgraded accordingly. Other upgrades are under study to further increase the acquisition speed, e.g., to double the number of Box-buses to gain a further factor two in the data transfer. Finally, some tests on DMA transfer may allow the FIFO memory readout time to be reduced to $60 \mu\text{s}$. This would not decrease dead time but would leave the CPU free to perform, for example, other monitoring tasks or data compression (zero-suppression). In conclusion, the performance of the first two cameras for the Phase I of H.E.S.S. is promising and, and are undergoing continual upgrades in order to optimize performance.